Chapter 3

Toy models for one-dimensional topological superconductors

In this chapter we will discuss two simple toy models for topological superconductors, i.e., superconductors whose Bogoliubov-de Gennes (BdG) Hamiltonian is topologically nontrivial. Both the Kitaev wire and the so-called $p + ip$ two-dimensional topological superconductor have nonlocal superconducting order parameters. We will set up the models, and show how the machinery of topological insulators can be applied to them. (1) They have bulk topological invariants, hence they cannot be adiabatically deformed to the atomic insulator limit. (2) They have edge states, that are topologically protected. (3) Bulk–boundary correspondence connects the number of edge states with the bulk topological invariants.

3.1 One-dimensional topological superconductor: the Kitaev Wire

The Kitaev wire is a toy model for a p-wave superconducting wire. It describes spinless fermions (e.g., spin polarized electrons) hopping on a chain consisting of N sites. The chain lies on top of a superconductor, which has a condensate of Cooper pairs. Thus, pairs of electrons on neighboring sites can hop off the chain simultaneously and form a Cooper pair in the superconductor. The inverse process can also occur: a Cooper pair in the superconductor can be broken, if the resulting fermions both end up in the chain, on neighboring sites. The grand

canonical Hamiltonian of this system reads,

$$\hat{H}_K = \sum_{m=1}^{N} \left(\frac{\epsilon_m}{2} \hat{c}_m^\dagger \hat{c}_m - w_m \hat{c}_m^\dagger \hat{c}_{m+1} + \Delta_m \hat{c}_{m+1}^\dagger \hat{c}_m^\dagger \right) + h.c. \tag{3.1}$$

The operator $\hat{c}_m$ annihilates an electron from site m. The first term describes the onsite potentials ϵ_m, which includes the chemical potential plus any site-dependent terms (e.g., electric potential from back-gates). The second term is the hopping of electrons between neighboring sites, with position-dependent amplitude w_m. The last term is the effect of superconductivity in the mean-field approximation, via the pair potential Δ_m, a set of complex parameters, corresponding to the wave function of the Cooper pair condensate. To calculate Δ_m self-consistently, we would need a description of the bulk superconductor, but in these notes, as in a large part of the literature, we treat Δ_m as parameters with no dynamics. In most of this chapter we will study the homogeneous case, with position independent hopping amplitude $w_m = w$ and pair potential $\Delta_m = \Delta$.

3.1.1 Bogoliubov-de Gennes Hamiltonian of the Kitaev wire: finite chain and bulk momentum-space Hamiltonian

We have seen in the previous chapter how the ground state, and the excitations of any superconductor can be described using a BdG Hamiltonian,

$$\hat{H} = \frac{1}{2} \begin{pmatrix} \hat{\mathbf{c}}^\dagger & \hat{\mathbf{c}} \end{pmatrix} \mathcal{H} \begin{pmatrix} \hat{\mathbf{c}} \\ \hat{\mathbf{c}}^\dagger \end{pmatrix} + \frac{1}{2} \mathrm{Tr} h; \qquad \mathcal{H} = \begin{pmatrix} h & \Delta \\ -\Delta^* & -h^* \end{pmatrix}, \tag{3.2}$$

with hermitian h and antisymmetric Δ matrices. This is the PHS-first-position-second basis for the BdG Hamiltonian, with, as an example, for the Kitaev wire for $N = 5$ sites, the matrices of the blocks that read

$$h = \begin{pmatrix} \epsilon_1 & -w_1 & 0 & w_N^* \\ -w_1^* & \epsilon_2 & \ddots & 0 \\ 0 & \ddots & \ddots & -w_{N-1} \\ -w_N & 0 & -w_{N-1}^* & \epsilon_N \end{pmatrix}; \quad \Delta = \begin{pmatrix} 0 & -\Delta_1 & 0 & \Delta_N \\ \Delta_1 & 0 & \ddots & 0 \\ 0 & \ddots & 0 & -\Delta_{N-1} \\ -\Delta_N & 0 & \Delta_{N-1} & 0 \end{pmatrix}.$$

To find the edge states and the bulk momentum-space BdG Hamiltonian of the Kitaev wire, it is worthwhile to reorder the creation and annihilation operators. Taking position first, particle-hole second, as

$$\underline{\hat{\mathbf{c}}}^\dagger = (\hat{c}_1^\dagger, \hat{c}_1, \hat{c}_2^\dagger, \hat{c}_2, \ldots, \hat{c}_N^\dagger, \hat{c}_N). \tag{3.3}$$

Using this shorthand, the BdG Hamiltonian reads,

$$\hat{H} = \frac{1}{2} \underline{\hat{\mathbf{c}}}^\dagger \mathcal{H} \underline{\hat{\mathbf{c}}}, \tag{3.4}$$

with

$$\mathcal{H} = \begin{pmatrix} \epsilon_1 & 0 & -w_1 & -\Delta_1 & 0 & 0 & 0 & 0 & -w_N^* & \Delta_N \\ 0 & -\epsilon_1 & \Delta_1^* & w_1^* & 0 & 0 & 0 & 0 & -\Delta_N^* & w_N \\ -w_1^* & \Delta_1 & \epsilon_2 & 0 & -w_2 & -\Delta_2 & 0 & 0 & 0 & 0 \\ -\Delta_1^* & w_1 & 0 & -\epsilon_2 & \Delta_2^* & w_2^* & 0 & 0 & 0 & 0 \\ 0 & 0 & -w_2^* & \Delta_2 & \epsilon_3 & 0 & -w_3 & -\Delta_3 & 0 & 0 \\ 0 & 0 & -\Delta_2^* & w_2 & 0 & -\epsilon_3 & \Delta_3^* & w_3^* & 0 & 0 \\ 0 & 0 & 0 & 0 & -w_3^* & \Delta_3 & \epsilon_4 & 0 & -w_4 & -\Delta_4 \\ 0 & 0 & 0 & 0 & -\Delta_3^* & w_3 & 0 & -\epsilon_4 & -\Delta_4^* & w_4 \\ -w_N & -\Delta_N & 0 & 0 & 0 & 0 & -w_3^* & \Delta_3 & \epsilon_N & 0 \\ \Delta_N^* & w_N^* & 0 & 0 & 0 & 0 & -\Delta_3^* & w_3 & 0 & -\epsilon_N \end{pmatrix};$$

Here, for an open chain, take $w_N = \Delta_N = 0$.

Particle-hole symmetry is here represented by the operator,

$$\hat{\mathcal{P}} = \underbrace{\sigma_x \oplus \sigma_x \oplus \ldots \oplus \sigma_x}_{N} \mathcal{K}, \tag{3.5}$$

where $\mathcal{K}$ is complex conjugation in position space.

3.1.2 Bulk momentum-space Hamiltonian

To find the bulk momentum-space Hamiltonian, we follow the same procedure as we did for the Su-Schrieffer-Heeger model. We start with the real-space matrix of the BdG Hamiltonian, Eq. (3.5), with translation invariance, $w_1 = w_2 = \ldots = w_N = |w| e^{i\chi} \in \mathbb{C}$, $\epsilon_1 = \epsilon_2 = \ldots = \epsilon_N = -\mu \in \mathbb{R}$, and $\Delta_1 = \Delta_2 = \Delta_N = \Delta \in \mathbb{C}$. We insert plane wave Ansatzes for the eigenvectors of this matrix, obtaining the eigenvalue equation,

$$\mathcal{H} \begin{pmatrix} u(k)e^{ik} \\ v(k)e^{ik} \\ u(k)e^{2ik} \\ v(k)e^{2ik} \\ u(k)e^{3ik} \\ v(k)e^{3ik} \\ u(k)e^{4ik} \\ v(k)e^{4ik} \\ u(k)e^{Nik} \\ v(k)e^{Nik} \end{pmatrix} = E(k) \begin{pmatrix} u(k)e^{ik} \\ v(k)e^{ik} \\ u(k)e^{2ik} \\ v(k)e^{2ik} \\ u(k)e^{3ik} \\ v(k)e^{3ik} \\ u(k)e^{4ik} \\ v(k)e^{4ik} \\ u(k)e^{Nik} \\ v(k)e^{Nik} \end{pmatrix}, \tag{3.6}$$

where $u(k)$ and $v(k)$ are the particle and hole components of the eigenmode. We can read off the Schrödinger equation for $u(k)$, $v(k)$ and $E(k)$, from, e.g., the third and fourth row of the above equation, as

$$\mathcal{H}(k) \begin{pmatrix} u(k) \\ v(k) \end{pmatrix} = E(k) \begin{pmatrix} u(k) \\ v(k) \end{pmatrix}, \tag{3.7}$$

with the matrix $\mathcal{H}(k)$ of the bulk momentum-space BdG Hamiltonian,

$$\mathcal{H}(k) = \begin{pmatrix} -2\,|w|\cos(k-\chi) - \mu & -2i\Delta \sin k \\ 2i\Delta^* \sin k & 2\,|w|\cos(k+\chi) + \mu \end{pmatrix}. \tag{3.8}$$

Particle-hole symmetry of the bulk momentum-space Hamiltonian reads

$$\hat{\sigma}_x \mathcal{K} \mathcal{H}(k) \mathcal{K} \hat{\sigma}_x = -\mathcal{H}(k). \tag{3.9}$$

Bear in mind here that $\mathcal{K}$ is complex conjugation in position space, and so,

$$\mathcal{K}\mathcal{H}(k)\mathcal{K} = \mathcal{H}(-k)^*, \tag{3.10}$$

where * denotes elementwise complex conjugation. You can verify using Eq. (3.8) that particle-hole symmetry is indeed fulfilled.

3.1.3 Bulk invariant: "polarization"

Similarly to the SSH model, the symmetry and the gap of the Hamiltonian induce quantization of the sum of the Berry phases of the negative-energy bands of the BdG Hamiltonian, $\sum_{n<0} \gamma_n$. For an ordinary band insulator, this would represent the bulk polarization, as we discussed last year.

This holds because the Berry phase of the nth positive energy and $-n$th negative energy band are equal. To show that, use particle-hole symmetry of the BdG Hamiltonian, i.e., if

$$\mathcal{H}(k)\,|n(k)\rangle = E_n(k)\,|n(k)\rangle\,, \tag{3.11}$$

then, acting with the particle-hole symmetry on both sides, we obtain

$$-\mathcal{H}(k)\hat{\sigma}_x\,|n(-k)\rangle^* = E_n(k)\hat{\sigma}_x\,|n(-k)\rangle^*\,. \tag{3.12}$$

Therefore, with a proper choice of gauge, we have

$$n > 0: \quad |n(k)\rangle = \hat{\sigma}_x\,|-n(-k)\rangle^*\,. \tag{3.13}$$

The gauge choice here involved fixing the phase of $|-n\rangle$ relative to the phase of $|n\rangle$. Now consider the integral needed to obtain the Berry phase across the Brillouin zone,

$$\begin{aligned} &\int_{-\pi}^{\pi} dk\,\langle n(k)|\,\partial_k\,|n(k)\rangle = \int_{-\pi}^{\pi} dk\,\langle -n(-k)|^*\,\hat{\sigma}_x\partial_k\hat{\sigma}_x\,|-n(-k)\rangle^* \\ &= \left(\int_{\pi}^{-\pi} dk\,\langle -n(k)|\,\partial_k\,|-n(k)\rangle\right)^* = \left(-\int_{-\pi}^{\pi} dk\,\langle -n(k)|\,\partial_k\,|-n(k)\rangle\right)^*. \end{aligned} \tag{3.14}$$

Since the integral above is purely imaginary, we obtain

$$\gamma_n = \frac{1}{2\pi i}\int_{-\pi}^{\pi} dk\,\langle n(k)|\,\partial_k\,|n(k)\rangle = \gamma_{-n}. \tag{3.15}$$

Thus,

$$\sum_{n<0} \gamma_n = \sum_{n>0} \gamma_n. \tag{3.16}$$

On the other hand, the sum of all Berry phases has to vanish,

$$\sum_{n<0} \gamma_n + \sum_{n>0} \gamma_n = 0 \pmod{2\pi}. \tag{3.17}$$

Thus, we have two options for this quantity, the BdG analogue of bulk polarization:

$$\text{trivial: } \sum_{n<0} \gamma_n = 0 \pmod{2\pi}; \tag{3.18}$$

$$\text{topological: } \sum_{n<0} \gamma_n = \pi \pmod{2\pi}. \tag{3.19}$$

A bulk topological invariant represents a *restriction*. Its nonzero value tells us that the Hamiltonian cannot be adiabatically deformed into an atomic insulating limit. By adiabatic deformation we mean a smooth, translation invariant change of the system parameters (possibly including the addition of new, longer range hopping terms), that respects the symmetries and keeps the bulk gap open. By atomic insulating limit we mean that the Hamiltonian is a direct sum of operators acting on the individual unit cells, no hopping.

The bulk polarization of the BdG Hamiltonian of a one-dimensional superconductor is a $\mathbb{Z}_2$ topological invariant. It can take on one of two distinct values (hence $\mathbb{Z}_2$), and thus cannot change under adiabatic deformation. In the atomic limit, obviously its value is 0. Thus if the polarization is π, we have a topological superconductor.

3.1.4 Edge states

We can find and analyze edge states in the BdG Hamiltonian of the Kitaev wire in the same way as we did for the SSH model.

1) Flat-band limit: edge states
2) Moving away from the flat-band limit: topological protection
3) General bulk–boundary correspondence argument: using polarization.

3.1.5 The Kitaev wire is more robust than the SSH model

The topological protection of the edge states in the SSH model depended on two fragile features: the robustness of the chiral symmetry and the indivisibility of the unit cell. An isolated edge state can be moved away from 0 energy by breaking chiral symmetry. This is easily realized, e.g., using an onsite potential. On the other hand, just changing the chain termination by adding an extra site is enough to move a bound state from 0 energy as well.

	Kitaev	SSH	Kitaev MF
PHS (+1)	$\sigma_x \mathcal{H}^* \sigma_x = -\mathcal{H}$	$\sigma_z H^*_{\mathrm{SSH}} \sigma_z = -H_{\mathrm{SSH}}$	$\mathcal{A}^* = \mathcal{A}$
TRS (+1)	$\mathcal{H}^* = \mathcal{H}$	$H^*_{\mathrm{SSH}} = H_{\mathrm{SSH}}$	$\sigma_z \mathcal{A}^* \sigma_z = -\mathcal{A}$
CS	$\sigma_x \mathcal{H} \sigma_x = -\mathcal{H}$	$\sigma_z H_{\mathrm{SSH}} \sigma_z = -H_{\mathrm{SSH}}$	$\sigma_z \mathcal{A} \sigma_z = -\mathcal{A}$

Table 3.1: The symmetries of the Kitaev wire and the Su–Schrieffer–Heeger (SSH) model. In the last column, the representation of the symmetries on the real matrix $\mathcal{A}$ representing the Kitaev wire with Majorana Fermions.

In the Kitaev wire, both the particle-hole symmetry and the indivisibility of the unit cell are hardwired into the formalism, and therefore are robust. Thus Majorana fermions as end states are more robust.

3.1.6 The Kitaev wire with real parameters is in the universality class of the SSH model

We might wonder whether the Kitaev wire – similarly to the SSH model – might possess a full $\mathbb{Z}$ invariant – a winding number – rather than just a $\mathbb{Z}_2$ invariant. Indeed, this is the case, if both the hopping amplitudes w_m and the pair potentials Δ_m are real. In that case the matrix of the real-space BdG Hamiltonian is real, and therefore possesses time-reversal symmetry, represented by complex conjugation.

In this case the fundamental symmetries of the Kitaev wire and the SSH model are listed in Table 3.1. They are the same, so we expect that with real parameters, the Kitaev wire can have any number of robust edge states at a single edge, not just 0 or 1.

The mapping is made explicit by a basis transformation

To bring out the similarities between the Kitaev wire and the SSH model, we can use a unitary rotation to map σ_x to σ_z. This is achieved by

$$\mathcal{H}' = e^{i\pi/4\,\sigma_y} \mathcal{H} e^{-i\pi/4\,\sigma_y} = \frac{1}{2} \begin{pmatrix} 1 & 1 \\ -1 & 1 \end{pmatrix} \mathcal{H} \begin{pmatrix} 1 & -1 \\ 1 & 1 \end{pmatrix}. \tag{3.20}$$

Substituting Eq. (1.39), this corresponds to

$$\mathcal{H}' = \begin{pmatrix} i(\operatorname{Im} h + \operatorname{Im} \Delta) & -\operatorname{Re} h + \operatorname{Re} \Delta \\ -\operatorname{Re} h - \operatorname{Re} \Delta & i(\operatorname{Im} h - \operatorname{Im} \Delta) \end{pmatrix}. \tag{3.21}$$

This is a Hermitian matrix because h is Hermitian and Δ is antisymmetric. The symmetries of $\mathcal{H}'$ are represented by the same operators as those of the SSH model.

For the bulk momentum-space Hamiltonian, taking $\operatorname{Im} \Delta = \operatorname{Im} w = 0$, we obtain

$$\mathcal{H}'(k) = \begin{pmatrix} 0 & -2w \cos k - \mu - 2i\Delta \sin k \\ -2w \cos k - \mu + 2i\Delta \sin k & 0 \end{pmatrix}. \tag{3.22}$$

Chapter 4

Two-dimensional topological superconductor

The simplest toy model for a two-dimensional topological superconductor is obtained by transcribing the Qi-Wu-Zhang model. The bulk momentum-space Hamiltonian of the Qi-Wu-Zhang model reads

$$\hat{H}_{QWZ}(k) = \begin{pmatrix} w\cos k_x + w\cos k_y + u & w\sin k_x + iw\sin k_y \\ w\sin k_x - iw\sin k_y & -w\cos k_x - w\cos k_y - u \end{pmatrix}, \quad (4.1)$$

where we used w for the enegy scale of the hopping amplitude. We can reinterpret this as a BdG Hamiltonian, introducing some extra parameters, as

$$\hat{H}_{p+ip}(k) = \begin{pmatrix} -w\cos k_x - w\cos k_y - \mu & -i\Delta_0\sin k_x + \Delta_0\sin k_y \\ i\Delta_0^*\sin k_x + \Delta_0^*\sin k_y & w\cos k_x + w\cos k_y + \mu \end{pmatrix}. \quad (4.2)$$

The superconducting order parameter in our toy model is not only nonlocal (p-wave), but also direction-dependent. There is a relative phase of i between the Cooper pairs created from $x-$ and $y-$ neighbors. For this reason, this model is called $p_x + ip_y$, or even shorter, $p + ip$. One might worry that this is not too realistic, and indeed, it is not clear whether it is actually realized in nature, although $SrRuO_4$ is a strong candidate.

The corresponding real-space lattice Hamiltonian reads,

$$\hat{H}_{p+ip} = \sum_{m,l=1}^{N} \Big(- w\hat{c}^\dagger_{m,l}\hat{c}_{m+1,l} - w\hat{c}^\dagger_{m,l}\hat{c}_{m,l+1} + h.c.\Big) - \mu \sum_{m,l=1}^{N} \hat{c}^\dagger_{m,l}\hat{c}_{m,l} + \sum_{m,l=1}^{N} \Big(\Delta_0\hat{c}^\dagger_{m+1,l}\hat{c}^\dagger_{m,l} + i\Delta_0\hat{c}^\dagger_{m,l+1}\hat{c}^\dagger_{m,l} + h.c.\Big). \quad (4.3)$$

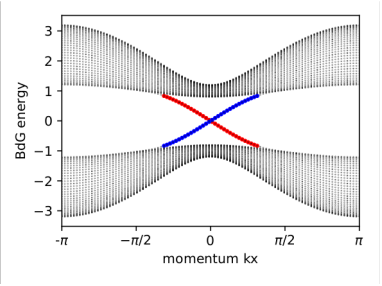

Figure 4.1: Dispersion relation of a strip of $p + ip$ superconductor. Red/blue are states localized on lower/upper edge (with 80% of probability within 2 sites of the boundary). Their wavefunction is equal weight particle and hole, within numerical accuracy.

4.1 Chern number, edge modes

We can apply everything we know about Chern insulators to this two-dimensional topological superconductor (maybe it is time for you to revise the first semester). This can be a gapped system with a bulk topological invariant: the Chern number Q, with

$$2w < \mu : \quad Q = 0; \tag{4.4a}$$
$$0 < \mu < 2w : \quad Q = 1; \tag{4.4b}$$
$$-2w < \mu < 0 : \quad Q = -1; \tag{4.4c}$$
$$\mu < -2w : \quad Q = 0. \tag{4.4d}$$

Correspondingly, in the gapped topological phases there are edge states, which propagate in one direction only along the edge. Such states are called "chiral".

The edge states are not Majorana zero modes, but Majorana fermions, branches of the dispersion relation whose negative-energy part is the particle-hole symmetric partner of the positive-energy part. They therefore have to cross $E = 0$ at either $k = 0$ or $k = \pi$. At the crossing point there is a state that is its own particle-home symmetry partner, and thus a Majorana zero mode.

To get more of an intuition for these Majorana fermion modes, we need to do an envelope function approximation for them, as we did for chiral edge modes of Chern insulators in the previous semester. We are looking for eigenstates of the linearized BdG Hamiltonian,

$$\begin{pmatrix} -\mu & \Delta(-\partial_x - i\partial_y) \\ \Delta^*(\partial_x - i\partial_y) & \mu \end{pmatrix} \begin{pmatrix} u(x,y) \\ v(x,y) \end{pmatrix} = E \begin{pmatrix} u(x,y) \\ v(x,y) \end{pmatrix}. \tag{4.5}$$

We take a setup with a boundary tilted at an angle θ with the y-axis (this also gives us an orientation). On the one side of the boundary is the sample, with $\mu > 0$ (trivial). On the other side of the boundary is the vacuum: in this equation, we can realize a vacuum by pushing up the dispersion relation of the electrons, taking μ to large negative values. For simplicity, we take $\Delta = |\Delta| e^{i\phi}$ to be constant. This would involve having a pair potential also in the vacuum, but since there is no density of states at 0 there anyway, this is not a problem.

For each energy E, we are looking for two eigenstates, that are plane-wave-like along the boundary, with wavenumbers to be specified. Actually, we will fix the wavenumber k, and find the corresponding energies E during the calculation; we will then verify if we have found two solutions for every energy. We take rotated coordinates to fit with the boundary:

$$x' = \cos\theta x - \sin\theta y; \qquad \partial_x = \cos\theta \partial_{x'} + \sin\theta\partial_{y'}; \tag{4.6}$$

$$y' = \cos\theta y + \sin\theta x; \qquad \partial_y = \cos\theta\partial_{y'} - \sin\theta\partial_{x'}, \tag{4.7}$$

where the equations on the right were derived using the chain rule, e.g., $\partial_x = \partial_x x'\partial_{x'} + \partial_x y'\partial_{y'}$. Substituting these and $-i\partial_{y'} = k$ into the BdG eigenvalue equation, we obtain

$$\begin{pmatrix} -\mu & \Delta e^{-i\theta}(-\partial_{x'} + k) \\ \Delta^* e^{i\theta}(\partial_{x'} + k) & \mu \end{pmatrix} \begin{pmatrix} u(x') \\ v(x') \end{pmatrix} = E \begin{pmatrix} u(x') \\ v(x') \end{pmatrix}. \tag{4.8}$$

We can now use an Ansatz:

$$u(x') = \pm e^{i(\phi-\theta)} v(x'). \tag{4.9}$$

Substituting this into the eigenvalue equation, we get a system of two equations:

$$\mp\mu e^{i(\phi-\theta)} v + k\Delta e^{-i\theta} v - \Delta e^{-i\theta}\partial_{x'} v = \pm E e^{i(\phi-\theta)} v; \tag{4.10}$$

$$\pm |\Delta| \partial_{x'} v \pm |\Delta| kv + \mu v = Ev. \tag{4.11}$$

Now taking $\pm e^{-i(\phi-\theta)}$ times the first equation plus and minus the second equation, we get

$$\pm |\Delta| k = E; \tag{4.12}$$

$$-2\mu v(x') \mp 2|\Delta| \partial_{x'} v(x') = 0. \tag{4.13}$$

The first equation shows us that these solutions are dispersionless chiral states propagating along the edge, in positive or negative direction. The second equation is solved by integration, and we obtain

$$\Psi(x', y') = \begin{pmatrix} \pm e^{i(\phi-\theta)} \\ 1 \end{pmatrix} \exp\left[\int_0^{x'} \frac{\pm\mu(x'')}{|\Delta|} dx''\right] e^{iky'}. \tag{4.14}$$

Although these are both eigenstates, only one of them is normalizable. When this is a left edge, i.e., $\mu > 0$ for $x' \to \infty$ and $\mu < 0$ for $x' \to -\infty$, it is the

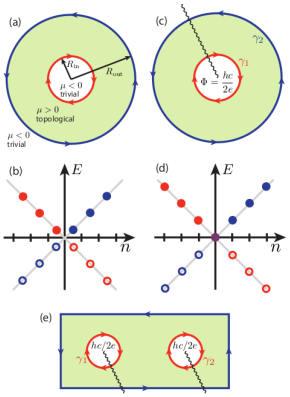

FIG. 4. (a) A topological $p + ip$ superconductor on an annulus supports chiral Majorana edge modes at its inner and outer boundaries. (b) Energy spectrum versus angular momentum n for the inner (red circles) and outer (blue circles) edge states in the setup from (a). Here n takes on half-integer values because the Majorana modes exhibit anti-periodic boundary conditions on the annulus. An $\frac{hc}{2e}$ flux piercing the central trivial region as in (c) introduces a branch cut (wavy line) which, when crossed, leads to a sign change for the Majorana edge modes. The flux therefore changes the boundary conditions to periodic and shifts n to integer values. This leads to the spectrum in (d), which includes Majorana zero-modes γ_1 and γ_2 localized at the inner and outer edges. The two-vortex setup in (e) supports one Majorana zero-mode localized around each puncture, while the outer boundary remains gapped.

Figure 4.2: Figure with caption from the review "New directions in the pursuit of Majorana fermions in solid state systems" by Jason Alicea

solution where the $\pm$ should be taken as $+$, a state propagating in the positive y' direction. On a right edge, i.e., $\mu < 0$ for $x' \to \infty$ and $\mu > 0$ for $x' \to -\infty$, it is the solution where the $\pm$ should be taken as $-$, a state propagating in the negative y' direction.

So for every energy E we have found only one edge state, propagating with velocity $|\Delta|$ along the boundary in a chiral way. The (Nambu) spinor $(u, v)^T$ describing the particle-hole structure of the Majorana edge modes is in the xy plane. Moreover, its angle follows the phase of the superconducting pair potential $\Delta(k)$, corresponding to the direction of propagation of the edge mode.

4.2 Majorana zero modes at the centers of magnetic vortices

If we take a sample of the $p+ip$ superconductor with a disk shape, we find chiral Majorana edge modes around the perimeter. These have allowed wavenumbers along the edge, which are quantized due to the finite size of the sample. They have to cross $E = 0$ at either $k = 0$ or $k = \pi$, and at the crossing point, there should be a Majorana Zero Mode. However, because of the finite size of the sample, wavenumber of the edge modes is quantized: not all wavenumbers are allowed, i.e., compatible with the boundary conditions around the perimeter. Is $k = 0$ an allowed wavenumber for Majorana edge modes on a disk?

Naively, one might expect that the boundary conditions for edge modes are periodic, and thus, $k = 0$, which respects these boundary conditions, is always allowed. However, chiral edge modes also have an internal degree of freedom, their particle-hole structure, which is analogous to a spin-half. And, just like with edge states of Chern insulators, their spin is oriented along the boundary. Therefore, after one round trip, this spin has turned around once, bringing a factor of (-1). Therefore, the boundary conditions required for Majorana fermions are in fact *antiperiodic*. Thus, no edge states at $k = E = 0$.

A way to create a Majorana Zero Mode edge state at $k = 0$ and $E \approx 0$ is to change boundary conditions for edge states by inserting a magnetic field through the middle of the disk. The magnetic field is shielded by the superconductor, falling off exponentially with the distance, with a characteristic London penetration depth λ, as in the Abrikosov vortices. Thus, far away from the vortex core, the magnetic field is no longer present. However, there is an Aharonov-Bohm phase picked up by the electrons, and this results in a twisting of the phase of the superconducting pair potential:

$$\text{vortex at } 0,\, r \gg \lambda\text{: } \Delta(x = r\cos\theta, y = r\sin\theta) = e^{i\Phi/\Phi_0\theta}\Delta(x = r, y = 0), \tag{4.15}$$

with Φ denoting the total magnetic flux in the vortex, and $\Phi_0 = e/(\pi\hbar)$ the superconducting flux quantum. Because the pair potential Δ has to be single valued, the magnetic flux inserted in a vortex has to be an integer multiple of the flux quantum.

We can now understand why, for a large disk, inserting a flux quantum through the middle of the disk brings with it a Majorana zero mode on the boundary, at $k = 0$. The Nambu spinor of the edge mode should rotate as we go around the perimeter, because it follows the phase of the pair potential, which follows the direction of propagation along the edge - one rotation for one round trip. However, introducing an odd number of flux quanta in a vortex in the middle of the disk results in an odd number of extra rotations – altogether, an even number of rotations of the spinor, and thus, no extra phase of -1. Hence, not antiperiodic, but periodic boundary conditions.

4.2.1 Gauge transformation

In a numerical model, it is convenient to do a gauge transformation to represent the effects of the vortex with less numerical effort. A gauge transformation changes the phases of terms in a lattice Hamiltonian, such as Eq. (4.3), in such a way that the spectrum is invariant. We start with a real phase field, $\Lambda_{\mathbf{r}} = \Lambda_{m,l} \in \mathbb{R}$, and we transform the creation and annihilation operators,

$$\hat{c}_{\mathbf{r}} \to \hat{c}_{\mathbf{r}} e^{i\Lambda_{\mathbf{r}}}; \qquad \hat{c}^\dagger_{\mathbf{r}} \to \hat{c}^\dagger_{\mathbf{r}} e^{-i\Lambda_{\mathbf{r}}}. \tag{4.16}$$

If we do this transformation of the Hamiltonian, the spectrum does not change: the same Bogoliubov tranformation diagonalizes the Hamiltonian as before, only

in terms of the transformed operators. Formulated differently: the above transformation is a unitary tranformation on the BdG Hamiltonian, and therefore does not change the spectrum.

The gauge transformation above can also be realized on the amplitudes of the hopping and superconducting terms in the lattice Hamiltonian. We therefore learn that the following transformation,

$$w_{\mathbf{r}',\mathbf{r}}\hat{c}^\dagger_{\mathbf{r}'}\hat{c}_{\mathbf{r}}; \quad w_{\mathbf{r}',\mathbf{r}} \to w_{\mathbf{r}',\mathbf{r}}e^{-i(\Lambda_{\mathbf{r}}-\Lambda_{\mathbf{r}})}; \tag{4.17}$$

$$\Delta_{\mathbf{r}',\mathbf{r}}\hat{c}^\dagger_{\mathbf{r}'}\hat{c}^\dagger_{\mathbf{r}}; \quad \Delta_{\mathbf{r}',\mathbf{r}} \to \Delta_{\mathbf{r}',\mathbf{r}}e^{-i(\Lambda_{\mathbf{r}}+\Lambda_{\mathbf{r}'})}, \tag{4.18}$$

does not change the spectrum.

When we represent the effects of a vortex carrying one quantum of magnetic flux, we could include the phase of the pair potential Δ explicitly, but it is more convenient to transform it out, using

$$\Lambda(x = r\cos\theta, y = r\sin\theta) = \theta. \tag{4.19}$$

As a result, the phase of the superconductor is uniform. However, all hoppings and pair potentials crossing the line going from the origin to positive infinity along x obtain an extra factor of -1, according to the rules of gauge transformation above. This gives us another way to see that the boundary conditions along the edge change from antiperiodic to periodic as flux quanta are threaded through the center of the disk.

4.2.2 Majorana zero mode at the vortex core

The core of a vortex with odd number of superconducting flux quanta hosts a Majorana zero mode. We can understand this by starting with a Corbino geometry, as in Fig. 4.2. The core is obtained by letting the radius of the inner (red) circle go to zero. In the case with an odd number of flux quanta threading the ring, there is always a Majorana zero mode there with $k = 0$, which has to remain there even if the size of the inner circle is 0.